AIP Physics of Plasmas

Particle-in-cell simulations of magnetic reconnection in laser-plasma experiments on Shenguang-II facility

San Lu, Quanming Lu, Quanli Dong, Can Huang, Shui Wang et al.

Citation: Phys. Plasmas 20, 112110 (2013); doi: 10.1063/1.4832015
View online: http://dx.doi.org/10.1063/1.4832015
View Table of Contents: http://pop.aip.org/resource/1/PHPAEN/v20/i11
Published by the AIP Publishing LLC.

Particle-in-cell simulations of magnetic reconnection in laser-plasma experiments on Shenguang-II facility

San Lu,[1] Quanming Lu,[1,a)] Quanli Dong,[2] Can Huang,[1] Shui Wang,[1] Jianqiang Zhu,[3] Zhengming Sheng,[4] and Jie Zhang[4]
[1]*CAS Key Laboratory of Geospace Environment, Department of Geophysics and Planetary Science, University of Science and Technology of China, Hefei 230026, China*
[2]*School of Physics and Optoelectronic Engineering, Ludong University, Yantai 264025, China*
[3]*CAS Key Laboratory for High Power Laser Physics, Chinese Academy of Sciences, Shanghai 201800, China*
[4]*Key Laboratory for Laser Plasmas (MoE) and Department of Physics, Shanghai Jiao Tong University, Shanghai 200240, China*

(Received 30 July 2013; accepted 5 November 2013; published online 19 November 2013)

Recently, magnetic reconnection has been realized in high-energy-density laser-produced plasmas. Plasma bubbles with self-generated magnetic fields are created by focusing laser beams to small-scale spots on a foil. The bubbles expand into each other, which may then drive magnetic reconnection. The reconnection experiment in laser-produced plasmas has also been conducted at Shenguang-II (SG-II) laser facility, and the existence of a plasmoid was identified in the experiment [Dong *et al.*, Phys. Rev. Lett. **108**, 215001 (2012)]. In this paper, by performing two-dimensional (2-D) particle-in-cell simulations, we investigate such a process of magnetic reconnection based on the experiment on SG-II facility, and a possible explanation for the formation of the plasmoid is proposed. The results show that before magnetic reconnection occurs, the bubbles squeeze strongly each other and a very thin current sheet is formed. The current sheet is unstable to the tearing mode instability, and we can then observe the formation of plasmoid(s) in such a multiple X-lines reconnection.
[http://dx.doi.org/10.1063/1.4832015]

I. INTRODUCTION

Magnetic reconnection, as a kind of energy conversion mechanism, is widely used to explain many explosive phenomena in solar atmosphere,[1–3] the Earth's magnetosphere,[4–6] laboratory experiments,[7,8] and even the magnetotail of a non-magnetized planet.[9,10] During magnetic reconnection, the topological structures of magnetic field lines are also rearranged. Thus, the stored magnetic energy is rapidly converted into plasma kinetic and thermal energies.[11–14] Plasmoid, which is also named magnetic island, is one of most important ingredients in magnetic reconnection. It was first predicted in the Near-Earth Neutral Line (NENL) magnetopheric model of the near-earth plasma sheet,[15,16] and hereafter observed for numerous times by satellites.[17–19] In general, the formation of a plasmoid can readily be understood in terms of simultaneous reconnection with multiple X-lines in plasma sheet.[20–22] Plasmoid is believed to be responsible for the high-energy electrons of magnetic reconnection. Electrons can be trapped by the plasmoid and accelerated until they gain sufficient energy and then escape, which is verified by recent particle-in-cell (PIC) simulations.[23–25] There are also observational evidences showing the enhancement of the energetic electron fluxes inside a plasmoid.[26–30] Recently, fully kinetic simulations with open boundary conditions found that plasmoid is also able to be generated in the elongated electron diffusion region of magnetic reconnection.[31] This kind of plasmoid which is embedded in the reconnection electron diffusion region is called secondary (magnetic) island,[32,33] which has also recently been observed by Cluster.[26–28,34]

Magnetic reconnection has also been realized in many dedicated laboratory experiments, such as magnetic reconnection experiment (MRX),[35] Versatile Toroidal Facility (VTF),[36] and Todai Spheromark-3/4(TS-3/4).[37,38] Besides these facilities, the high-energy-density (HED) laser-driven experiment provides a new platform to study magnetic reconnection. In such experiment, two expanding plasma bubbles are created by two closely focusing laser beams on a planer foil target, and then the azimuthal magnetic fields are self-generated through noncollinear electron density and temperature gradients ($\nabla n_e \times \nabla T_e$) around the laser spots.[39] If the bubbles with the opposing magnetic fields eventually encounter each other, magnetic reconnection may occur between the two approaching plasma bubbles. The experimental measurements of the magnetic fields and plasma dynamics in such geometry were firstly carried out by Nilson *et al.*,[40] and then Li *et al.*[41] made further observations. In their studies, highly collimated bidirectional plasma jets and topological changes of magnetic field were observed, which indicated the occurrence of magnetic reconnection. After the experimental observations of magnetic reconnection in HED laser-produced plasmas, Fox *et al.*[42,43] performed two-dimensional (2-D) PIC simulations to study the reconnection between the plasma bubbles with parameters and geometry relevant to these experiments. It was found that the high

[a)]Author to whom correspondence should be addressed. Email: qmlu@ustc.edu.cn

reconnection rate which is faster than the prediction by the classic Hall-MHD theory in such a strongly driven system can be explained by substantial flux-pileup effects, which enhances the relevant magnetic field intensity at the shoulder of the current sheet. In the simulations with the Omega experiment parameters, Fox *et al.*[43] found that the current sheet was broken into several islands, and they indicated that these islands are generated due to tearing mode instability or Rayleigh-Taylor-like instabilities.[43]

In recent experiment conducted on Shenguang-II (SG-II) laser facility, a plasmoid was also observed during reconnection in laser-produced plasmas.[44] In this paper, by performing 2-D PIC simulations, magnetic reconnection between two expanding plasma bubbles is investigated, with parameters and geometry based on the reported SG-II experiment.[44] The generation of the plasmoid observed in the reconnection experiment on SG-II facility is attributed to the tearing mode instability, which is unstable in a thin current sheet. Such a current sheet is formed when the plasma bubbles created by two closely focusing laser beams on a planer foil target squeeze each other strongly.

The paper is organized as follows. In Sec. II, the simulation setup based on experimental parameters is described. Section III presents the simulation results, which focus on the process of magnetic reconnection and plasmoid generation between two expanding plasma bubbles. Section IV gives the conclusions.

II. SIMULATION SETUP

Based on the SG-II experimental setup, 2-D PIC simulation model is employed to study the formation mechanism of a plasmoid during magnetic reconnection in laser-produced plasmas. In our 2-D PIC simulation model, the electromagnetic fields are defined on the grids and updated by solving the Maxwell equations with a full explicit algorithm. The ions and electrons are advanced in the electromagnetic field. The initial configuration of the simulation system is two expanding semicircular plasma bubbles, which is in accord with the previous PIC simulations by Fox *et al.*[42,43] The computation is carried out in a rectangular domain in the $(x,\ z)$ plane with the dimension $[-L_x, L_x] \times [-L_z, L_z]$. The two semicircular bubbles centered at $(0, -L_z)$ and $(0, L_z)$, respectively. The radius vectors of the bubbles are defined from the center of each bubble, which can be expressed as $\mathbf{r}^{(1)} = (x, z + L_z)$ and $\mathbf{r}^{(2)} = (x, z - L_z)$. The initial number density is $n_b + n^{(1)} + n^{(2)}$, where n_b is a background density, and $n^{(i)} (\mathrm{i} = 1,\ 2)$ is

$$n^{(i)} = \begin{cases} (n_0 - n_b)\cos^2\left(\dfrac{\pi r^{(i)}}{2L_n}\right) & \text{if } r^{(i)} < L_n \\ 0 & \text{otherwise,} \end{cases} \tag{1}$$

where L_n is the initial scale of the bubbles, and n_0 is the peak bubble density. Initially, the bubbles are expanding radially, and the velocity is expressed as the sum of the following fields:

$$\mathbf{V}^{(i)} = \begin{cases} V_0 \sin\left(\dfrac{\pi r^{(i)}}{L_n}\right)\hat{\mathbf{r}}^{(i)} & \text{if } r^{(i)} < L_n, \\ 0 & \text{otherwise,} \end{cases} \tag{2}$$

where V_0 is the initial expanding speed of the two plasma bubbles. The magnetic field is initialized as the sum of two toroidal ribbons, with

$$\mathbf{B}^{(i)} = \begin{cases} B_0 \sin\left(\dfrac{\pi(L_n - r^{(i)})}{2L_B}\right)\hat{\mathbf{r}}^{(i)} \times \hat{\mathbf{y}} & \text{if } r^{(i)} \in [L_n - 2L_B, L_n], \\ 0 & \text{otherwise.} \end{cases} \tag{3}$$

Here, B_0 is the initial strength of the magnetic field, and L_B is the half-width of the magnetic ribbons. An initial electric field $\mathbf{E} = -\mathbf{V} \times \mathbf{B}$ is added in order to be consistent with the plasma flow, and the initial out-of-plane current density is determined by Faraday's Law.

In order to simulate the reconnection experiment on SG-II facility, our PIC simulation parameters are chosen based on the reported or estimated SG-II experimental parameters, which are listed in Table I.[41] In the experiment, the measured electron density is about $5 \times 10^{19}\mathrm{cm}^{-3}$ near the X-line; and here, we assume $n_0 = 10 n_b$. Therefore, the peak electron density is about $5 \times 10^{20}\mathrm{cm}^{-3}$. The electron temperature is measured to be $T_e \sim 570\mathrm{eV}$, and the ion temperature is assumed to be same as the electron temperature, $T_i \sim T_e$. The estimated average ionic charge is about 10, and thus the peak ion density is about $5 \times 10^{19}\mathrm{cm}^{-3}$. The ion inertial length based on the peak ion density is about $d_i = c/\omega_{pi} = 16.8\,\mu\mathrm{m}$. The plasma bubble radius is about $L_n = 200\,\mu\mathrm{m}$, and the width of the magnetic ribbons $2L_B$ is about $80\,\mu\mathrm{m}$. In our PIC simulations, we choose $L_n = 12 d_i$, and $L_B = 2 d_i$. In the experiment, the magnetic field is estimated to be around 3.75 MG. However, it is a value in the pileup region after the bubbles are strongly squeezed, where the magnetic field can be enhanced 4–6 times. Therefore, in the simulations, we choose $B_0 = 0.8\mathrm{MG}$. The mass ratio m_i/m_e is set to be 100 and the light speed c is $150 v_A$ (where v_A is the Alfvén speed based on B_0 and n_{i0}). The initial

TABLE I. SG-II experimental parameters.[41]

Parameter		Reported or estimated values
Ions		Al
Average ionic charge	Z	$\sim$10
Peak electron density	n_{e0}	$\sim 5 \times 10^{20}\ \mathrm{cm}^{-3}$
Peak ion density	n_{i0}	$5 \times 10^{19}\ \mathrm{cm}^{-3}$
Plasma bubble scale	L_n	$200\ \mu\mathrm{m}$
Width of magnetic ribbon	$2L_B$	$80\ \mu\mathrm{m}$
Temperature	T_e, T_i	570 eV
Magnetic field	B_0	0.8 MG
Estimated inflow speed	V_0	$5.4 \times 10^5\ \mathrm{m/s}$
Ion inertial length	$d_i = c/\omega_{pi}$	$16.8\ \mu\mathrm{m}$
Alfvén speed	v_A	$4.7 \times 10^4\ \mathrm{m/s}$
Electron beta	β_e	18
Sound speed	$C_s = (\gamma Z T_e/m_i)^{1/2}$	$1.8 \times 10^5\ \mathrm{m/s}$

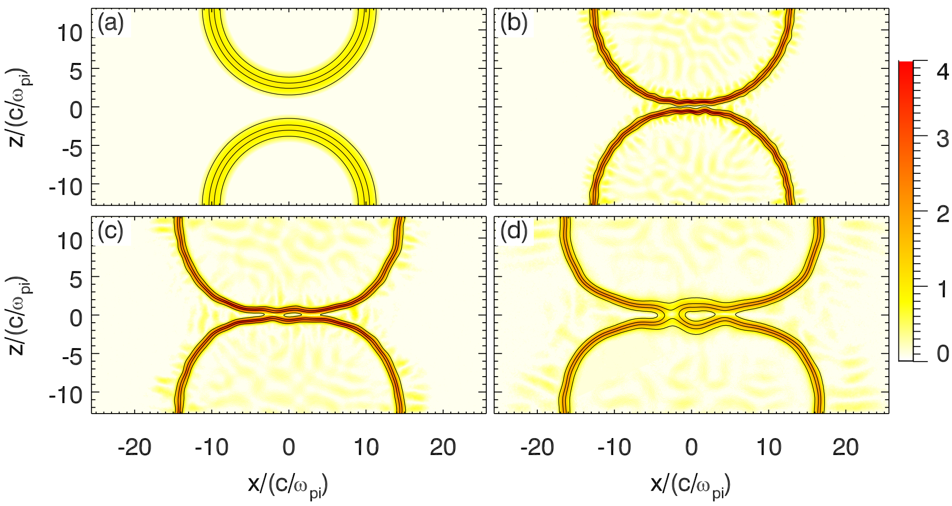

FIG. 1. The contours of the magnitude of the magnetic field B/B_0 at $\Omega_i t =$ (a) 0, (b) 0.44, (c) 0.7, and (d) 1.2. The magnetic field lines are also plotted in the figure for reference.

distribution functions for the ions and electrons are Maxwellian with the bulk velocities in the radial direction (described by Eq. (2)) and drift velocities in the y direction, which supply the out-of-plane current. In the simulations, uniform initial ion and electron temperatures are adopted for simplicity, $T_{i0} = T_{e0} = 0.04 m_e c^2$. It is noteworthy that the sound speed $C_s = (\gamma Z T_e / m_i)^{1/2}$ is an important parameter in the system, because the expanding speed of the plasma bubbles V_0 is at the order of C_s. In the simulations, we choose $V_0 = 3C_s \approx 11.5 v_A$.

We set $L_x = 25.6 c/\omega_{pi}$ and $L_z = 12.8 c/\omega_{pi}$, and number of the grids is $N_x \times N_z = 1024 \times 512$ with spatial resolution $\Delta x = \Delta z = 0.05 c/\omega_{pi}$. The time step is $\Omega_i t = 0.0002$ ($\Omega_i = eB_0/m_i$ is the ion gyrofrequency). More than 2×10^8 particles per species are employed to simulate the plasmas. In the simulations, the periodic boundary conditions are used along both the x and z directions.

III. SIMULATION RESULTS

To simulate the SG-II reconnection experiment and investigate the generation of plasmoid in laser-produced plasmas, a simulation with the parameters identified to those of the experiment is performed in this paper. Figure 1 shows the contours of the magnetic field B/B_0, with (a), (b), (c), and (d) representing the time $\Omega_i t = 0$, 0.44, 0.7, and 1.2, respectively. The magnetic field lines are also plotted in the figure for reference. Panel (a) corresponds to the magnetic field at the initial time. At $\Omega_i t = 0.44$, the plasma bubbles begin to squeeze each other strongly by the supersonic expansion, and the magnetic field wrapping around the plasma bubbles is enhanced. The maximum value of the magnetic field is about four times that of the initial time. At the center of the simulation domain, a thin current sheet is formed when the two expanding plasma bubbles encounter and squeeze each other. At $\Omega_i t = 0.7$, two reconnection X-lines are formed, and a plasmoid is generated between the X-lines. As the reconnection develops, the plasmoid grows larger and gradually moves to the right until it merges with the magnetic field in the outflow region (Fig. 1(d)). A more detailed evolution of the current sheet is presented in Fig. 2. In the figure, contours of the out-of-plane current density $J_y/(en_0 v_A)$ at $\Omega_i t =$ (a) 0.44, (b) 0.52, (c) 0.76, and (d) 1.2 are plotted. Obviously, a thin current sheet is formed before the reconnection occurs, and then the plasmoid is generated.

According to the linear theory,[45,46] the tearing mode instability is unstable in a current sheet when $k\delta < 1$, and the maximum growth rate occurs at $k\delta = 0.55$, where k is the wave number of the tearing mode instability, and δ is the half-width of the current sheet. In the 2-D regime, the tearing mode instability is widely believed to be the onset mechanism of magnetic reconnection.[47,48] If the number of the reconnection X-lines, $M = \frac{L}{2\pi} k$, is greater than or equal to two, plasmoid(s) can be formed due to the tearing mode instability. The length (L) and half-width (δ) of the current sheet are crucial for the formation of plasmoid. We can

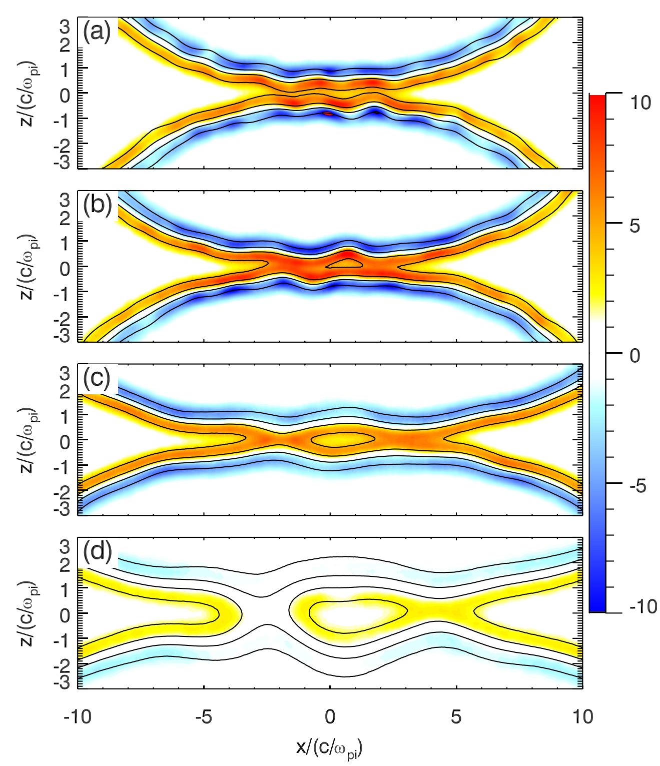

FIG. 2. The zoom-in contours of the out-of-plane current density $J_y/(en_0 v_A)$ at $\Omega_i t =$ (a) 0.44, (b) 0.52, (c) 0.76, and (d) 1.2. The magnetic field lines are also plotted in the figure for reference.

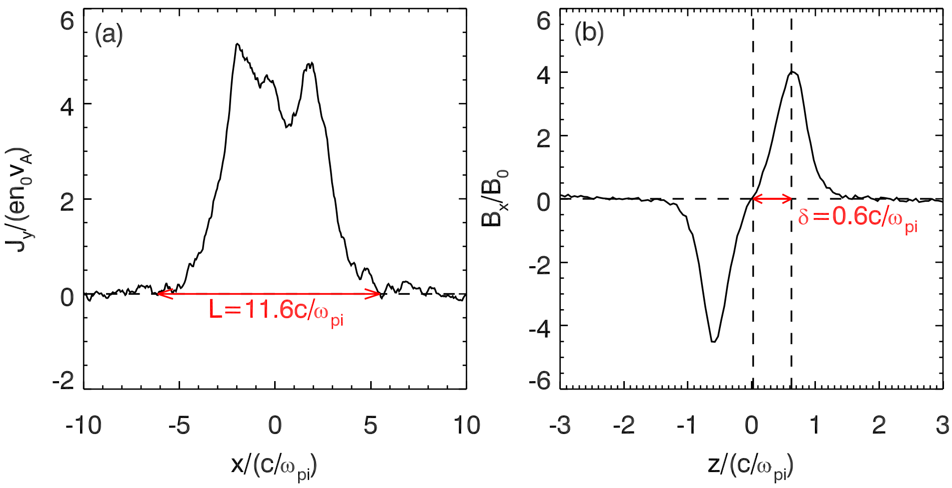

FIG. 3. The definitions of the length (L) and half-width (δ) of the current sheet. The length of the current sheet is defined as the length of the region where the value of the out-of-plane current density larger than zero along $z=0$. The width of the current sheet is defined as the distance between the positive and negative peaks of B_x along $x=0$. According to the definitions, at the time $\Omega_i t=0.44$ which is just before the beginning of the tearing mode instability, (a) the length of the current sheet is $L=11.6c/\omega_{pi}$, (b) the half-width of the current sheet is $\delta=0.6c/\omega_{pi}$.

calculate the length and half-width of the current sheet. The length of the current sheet is defined as the length of the region where the value of the out-of-plane current density larger than zero along the line $z=0$, while the width of the current sheet is defined as the distance between the positive and negative peaks of B_x along the line $x=0$, which are shown in Fig. 3.

Figure 4 shows the evolution of the length and half-width of the current sheet. As the plasma bubbles expand and squeeze each other, the length of the current sheet increases, and the half-width decreases. The reconnection onset occurs around $\Omega_i t=0.44$, at the time, the length and half-width of the current sheet are $L=11.6c/\omega_{pi}$ and $\delta=0.6c/\omega_{pi}$, respectively. According to the linear theory,[45,46] the maximum growth rate occurs at

$$k\delta = 2\pi M\frac{\delta}{L} = 0.55, \tag{4}$$

where $M=1,2,3,\ldots$. Therefore, the most unstable tearing mode is $M=2$ ($k\delta\approx 0.65$), which is consistent with our simulation results: two reconnection X-lines are grown in the current sheet, and a plasmoid is formed between the two X-lines.

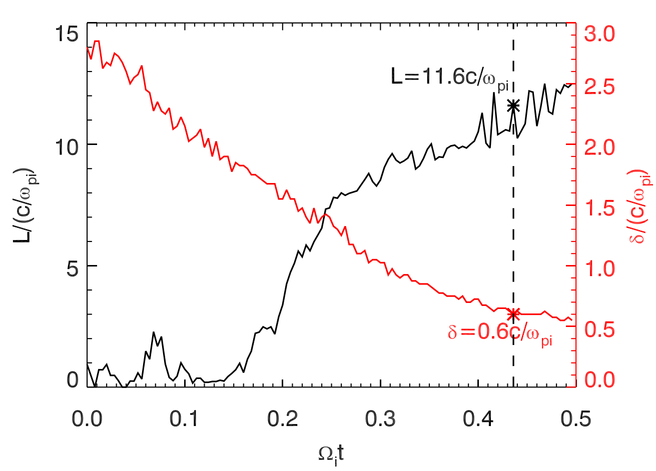

FIG. 4. The time evolution of the length (L) and half-width (δ) of the current sheet. The critical point just before the beginning of the tearing mode instability of the current sheet is marked by the vertical dashed line.

In summary, the process for the formation of plasmoid can be described as follows: in the first stage, the two bubbles expand supersonically and squeeze each other, which leads to the formation of a thin current sheet; in the second stage, the tearing mode instability is excited in such a thin current sheet, and a plasmoid is then generated. In order to verify the above conclusion, we run two additional cases, where we change the initial expanding speed of the plasma bubbles to $V_0=1.25C_s\approx 4.8v_A$ and $V_0=7.5C_s\approx 28.7v_A$, respectively. The other parameters are unchanged. Figure 5 shows the contours of the magnetic field B/B_0 for the case with $V_0=1.25C_s=5v_A$ at $\Omega_i t=$(a) 0, (b) 1.08, (c) 2, and (d) 3.8, respectively. At $\Omega_i t=$1.08, a current sheet begins to be formed. Then, a single X-line reconnection is initiated and developed in the center of the simulation domain. In this case, the magnetic field in the upstream pileup region is smaller (about $2B_0$), and the reconnection process is slower, which lasts about $4\Omega_i^{-1}$. Figure 6 plots the time evolution of the length and half-width of the current sheet for the case with $V_0=1.25C_s\approx 4.8v_A$. At the critical point ($\Omega_i t=$1.09), when the reconnection is about to occur, the length and the half-width of the current sheet is $L=11.65c/\omega_{pi}$ and $\delta=0.875c/\omega_{pi}$, respectively. Based on the linear theory of the tearing mode instability, the most unstable mode is $M=1$ ($k\delta\approx 0.47$). Therefore, we can only observe one X-line and no plasmoid is formed.

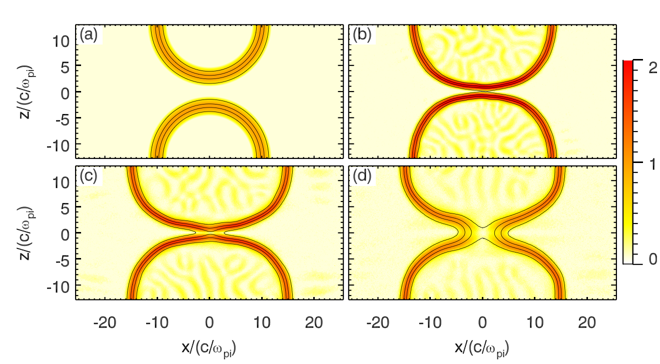

FIG. 5. The contours of the magnitude of the magnetic field B/B_0 for the run with low initial expanding speed $V_0=1.25C_s\approx 4.8v_A$ at $\Omega_i t=$(a) 0, (b) 1.08, (c) 2, and (d) 3.8. The magnetic field lines are also plotted in the figure for reference.

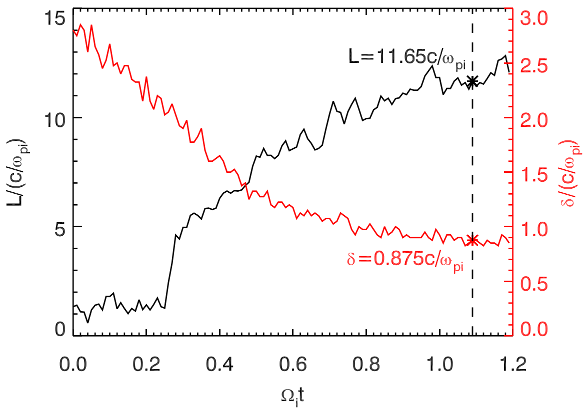

FIG. 6. The time evolution of the length (L) and half-width (δ) of the current sheet for the run with low initial expanding speed $V_0 = 1.25C_s \approx 4.8v_A$. The time just before the beginning of the tearing mode instability of the current sheet is marked by the vertical dashed line.

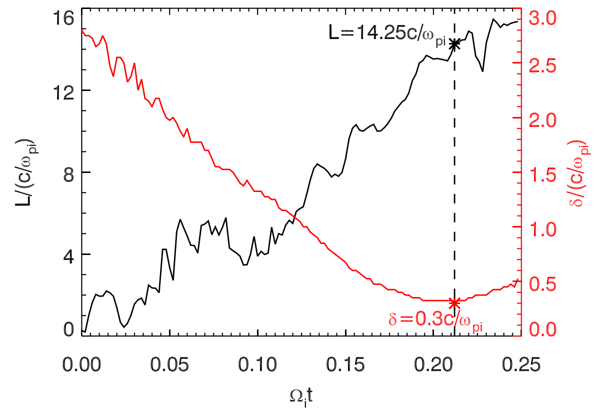

FIG. 8. The time evolution of the length (L) and half-width (δ) of the current sheet for the run with high initial expanding speed $V_0 = 7.5C_s = 28.7v_A$. The time just before the beginning of the tearing mode instability of the current sheet is marked by the vertical dashed line.

The contours of the magnetic field B/B_0 for the case with $V_0 = 7.5C_s \approx 28.7v_A$ are presented in Fig. 7, with (a), (b), (c), and (d) representing the time $\Omega_i t = 0$, 0.21, 0.3, and 0.35, respectively. Because of the high expanding speed, at $\Omega_i t = 0.21$, a very long and thin current sheet is formed between the two expanding and squeezing plasma bubbles, and the magnetic field in the upstream pileup region is very strong ($\sim 8B_0$). After this, four reconnection X-lines and three plasmoids are formed in the current sheet. Eventually plasmoids merge with the magnetic field in the outflow region. In the high expanding speed case, magnetic reconnection is faster, which last about $0.4\Omega_i^{-1}$. Figure 8 plots the time evolution of the length and half-width of the current sheet for the case with $V_0 = 7.5C_s = 30v_A$. Because of the high expanding speed of the bubbles, the resulting compressed current sheet becomes longer and thinner. The length and half-width of the current sheet just before the reconnection occurs ($\Omega_i t = 0.212$) are $L = 14.25c/\omega_{pi}$ and $\delta = 0.3c/\omega_{pi}$, respectively. According to the linear theory, the most unstable tearing mode of the current sheet is $M = 4$ ($k\delta \approx 0.53$), and four X-lines are formed in the case with high expanding speed. Therefore, there are three plasmoids formed in the current sheet.

IV. DISCUSSION AND CONCLUSIONS

Magnetic reconnection between HED plasma bubbles has recently been conducted on SG-II laser facility.[44] In this paper, 2-D PIC simulations are performed to investigate magnetic reconnection between two expanding plasma bubbles with parameters and geometry based on the reported SG-II experiment.[44] The results show that a thin current sheet is first formed between the two supersonically expanding plasma bubbles, and the tearing mode instability is unstable in such a current sheet. Subsequently, two X-lines are developed due to the tearing mode instability, and a plasmoid is formed. With the development of the reconnection, the plasmoid grows larger and gradually merge with the magnetic field in the outflow region. Our simulations provide a possible generation mechanism for the plasmoid observed in the reconnection experiment on SG-II facility.

Fox *et al.*[42,43] have shown that in a strongly driven reconnection regime, such as reconnection between laser-produced plasma bubbles, the magnetic flux will pileup in the inflow region when the inflow rate of the magnetic flux is much larger than the reconnection rate. The reconnection rate increases sharply with the pileup of the magnetic flux. Our simulations verify the results of Fox *et al.*[42,43] Furthermore, we find that when the expanding speed of the

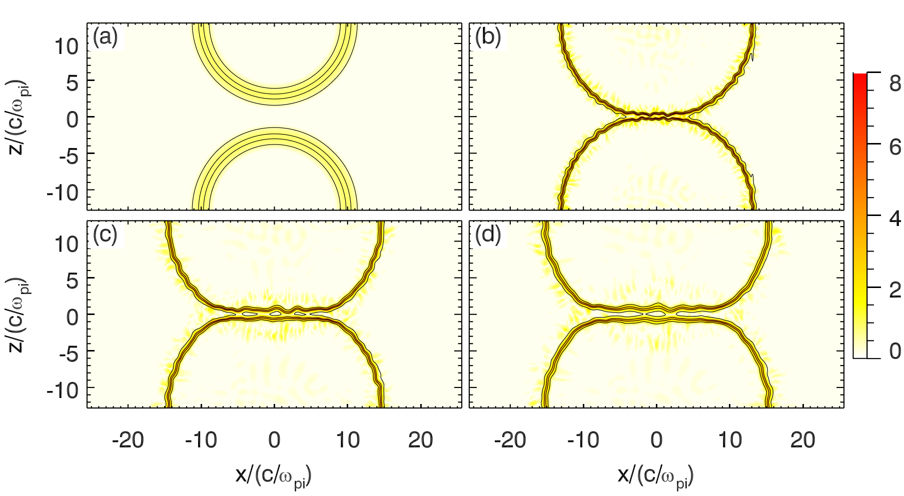

FIG. 7. The contour of the magnitude of the magnetic field B/B_0 for the run with high initial expanding speed $V_0 = 7.5C_s = 28.7v_A$ at $\Omega_i t =$ (a) 0, (b) 0.21, (c) 0.3, and (d) 0.35. The magnetic field lines are also plotted in the figure for reference.

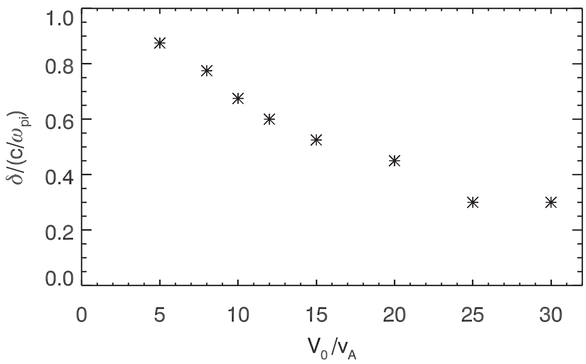

FIG. 9. Half-width of the current sheet (δ) versus initial expanding speed of the plasma bubbles (V_0). The half-width of the current sheet is measured at the time just before the beginning of the tearing mode instability.

plasma bubbles is sufficiently large, a thin current sheet, which is unstable to the tearing mode instability, is formed due to the strong squeeze of the plasma bubbles. Then, multiple X-lines reconnection occurs, and plasmoids are generated. Because the plasma bubbles expand with the velocity at the order of the sound speed and the reconnection rate is related to the Alfven speed, the magnetic flux in the inflow region will pileup and a thin current sheet may be formed when the plasma beta ($\beta_e = (C_s/v_A)^2$) is much larger than one. This can be seen more clearly in Fig. 9, which shows the relation between the half-width (δ) of the current sheet when the reconnection just begins to occur and the expanding speed (V_0) of the plasma bubbles. Obviously, with the increase of the expanding speed, the half-width of the current sheet decrease. Our simulations are also consistent with the results of Fox *et al.*[43] When they performed the simulations with the Omega experiment parameters (where the plasma beta is about 150), several islands are observed in the current sheet, while there is no generation of plasmoids in the simulations with the Rutherford experiment parameters (where the plasma beta is about 8).

The Rayleigh-Taylor instability may be unstable in the laser-produced plasma bubbles, which is wrapped with the curved magnetic field. Fox *et al.*[43] indicated that the Rayleigh-Taylor instability may play an important role in the generation of plasmoid during magnetic reconnection between HED plasma bubbles. However, the wave vector of the instability are generally perpendicular to both the background magnetic field and the centrifugal force acting on the plasma due to particle motions along the curved magnetic field.[49] It is along the y direction, which is neglected in our simulations. A three-dimensional (3-D) model is necessary for investigating the role of the Rayleigh-Taylor instability during magnetic reconnection between HED plasma bubbles, which is our future goal.

ACKNOWLEDGMENTS

This research was supported by the 973 Program (2013CBA01503 and 2012CB825602), the National Science Foundation of China, Grant Nos. 11235009, 41174124, 41274144, and 41121003, CAS Key Research Program KZZD-EW-01, and Ministry of Education (Grant No. IRT1190).

[1] R. G. Giovanelli, Nature (London) **158**, 81 (1946).
[2] S. Tsuneta, H. Hara, T. Shimizu, L. W. Acton, K. T. Strong, H. S. Hudson, and Y. Ogawara, Publ. Astron. Soc. Jpn. **44**, L63 (1992).
[3] B. V. Somov and T. Kosugi, Astrophys. J. **485**, 859 (1997).
[4] D. N. Baker, T. I. Pulkkinen, V. Angelopoulos, W. Baumjohann, and R. L. McPherron, J. Geophys. Res. **101**, 12975, doi:10.1029/95JA03753 (1996).
[5] T. Nagai, M. Fujimoto, Y. Saito, S. Machida, T. Terasawa, R. Nakamura, T. Yamamoto, T. Mukai, A. Nishida, and S. Kokubun, J. Geophys. J. **103**, 4419 (1998).
[6] V. Angelopoulos, J. P. McFadden, D. Larson, C. W. Carlson, S. B. Mende, H. Frey, T. Phan, D. G. Sibeck, K. H. Glassmeier, U. Auster, E. Donovan, I. R. Mann, I. J. Rae, C. T. Russell, A. Runov, X. Z. Zhou, and L. Kepko, Science **321**, 931 (2008).
[7] J. Wesson, *Tokomaks* (Oxford University Press, New York, 1997).
[8] H. T. Ji, M. Yamada, S. Hsu, and R. Kulsrud, Phys. Rev. Lett. **80**, 3256 (1998).
[9] J. P. Eastwood, D. A. Brain, J. S. Halekas, J. F. Drake, T. D. Phan, M. Oieroset, D. L. Mitchell, R. P. Lin, and M. Acuna, Geophys. Res. Lett. **35**, L02106, doi:10.1029/2007GL032289 (2008).
[10] T. L. Zhang, Q. M. Lu, W. Baumjohann, C. T. Russell, A. Fedorov, S. Barabash, A. J. Coates, A. M. Du, J. B. Cao, R. Nakamura, W. L. Teh, R. S. Wang, X. K. Dou, S. Wang, K. H. Glassmeier, H. U. Auster, and M. Balikhin, Science **336**, 567 (2012).
[11] D. Biskamp, *Magnetic Reconnection in Plasmas* (Cambridge University Press, Cambridge, 2000).
[12] J. Birn and E. R. Priest, *Reconnection of Magnetic Fields: Magnetohydrodynamics and Collisionless Theory and Observations* (Cambridge University Press, Cambridge, 2007).
[13] M. Yamada, R. Kulsrud, and H. T. Ji, Rev. Mod. Phys. **82**, 603 (2010).
[14] S. Lu, Q. M. Lu, C. Huang, and S. Wang, Phys. Plasmas **20**, 061203 (2013).
[15] E. W. Hones, Jr., in *Physics of Solar Planetary Environments*, edited by D. J. Williams (AGU, Washington DC, 1976), p. 558.
[16] E. W. Hones, Jr., Space Sci. Rev. **23**, 393 (1979).
[17] R. C. Elphic, C. A. Cattell, K. Takahashi, S. J. Bame, and C. T. Russell, Geophys. Res. Lett. **13**, 648, doi:10.1029/GL013i007p00648 (1986).
[18] Q. G. Zong, T. A. Fritz, Z. Y. Pu, S. Y. Fu, D. N. Baker, H. Zhang, A. T. Lui, I. Vogiatzis, K. H. Glassmeier, A. Korth, P. W. Daly, A. Balogh, and H. Reme, Geophys. Res. Lett. **31**, L18803, doi:10.1029/2004GL020692 (2004).
[19] S. M. Imber, J. A. Slavin, H. U. Auster, and V. Angelopoulos, J. Geophys. Res. **116**, A02201, doi:10.1029/2010JA016026 (2011).
[20] J. A. Slavin, R. P. Lepping, J. Gjerloev, D. H. Fairfield, M. Hesse, C. J. Owen, M. B. Moldwin, T. Nagai, A. Ieda, and T. Mukai, J. Geophys. Res. **108**, 1015, doi:10.1029/2002JA009557 (2003).
[21] H. Hasegawa, J. Wang, M. W. Dunlop, Z. Y. Pu, Q. H. Zhang, B. Lavraud, M. G. G. T. Taylor, O. D. Constantinescu, J. Berchem, V. Angelopoulos, J. P. McFadden, H. U. Frey, E. V. Panov, M. Volwerk, and Y. V. Bogdanova, Geophys. Res. Lett. **37**, L16101, 10.1029/2010GL044219 (2010).
[22] M. Øieroset, T. D. Phan, J. P. Eastwood, M. Fujimoto, W. Daughton, M. A. Shay, V. Angelopoulos, F. S. Mozer, J. P. McFadden, D. E. Larson, and K. H. Glassmeier, Phys. Rev. Lett. **107**, 165007 (2011).
[23] J. F. Drake, M. Swisdak, H. Che, and M. A. Shay, Nature **443**, 553 (2006).
[24] X. R. Fu, Q. M. Lu, and S. Wang, Phys. Plasmas **13**, 012309 (2006).
[25] M. Oka, M. Fujimoto, I. Shinohara, and T. D. Phan, J. Geophys. Res. **115**, A08223, doi:10.1029/2010JA015392 (2010).
[26] R. S. Wang, Q. M. Lu, A. M. Du, and S. Wang, Phys. Rev. Lett. **104**, 175003 (2010).
[27] R. S. Wang, Q. M. Lu, X. Li, C. Huang, and S. Wang, J. Geophys. Res. **115**, A11201, doi:10.1029/2010JA015473 (2010).
[28] R. S. Wang, R. Nakamura, Q. M. Lu, A. M. Du, T. L. Zhang, W. Baumjohann, Y. V. Khotyaintsev, M. Volwerk, M. André, M. Fujimoto, T. K. M. Nakamura, A. N. Fazakerley, J. Du, W. Teh, E. V. Panov, B. Zieger, Y. X. Pan, and S. Lu, J. Geophys. Res. **117**, A07223, doi:10.1029/2011JA017384 (2012).
[29] L. J. Chen, A. Bhattacharjee, P. A. Puhl-Quinn, H. Yang, N. Bessho, S. Imada, S. Mühlbachler, P. W. Daly, B. Lefebvre, Y. Khotyaintsev, A. Vaivads, A. Fazakerley, and E. Georgescu, Nat. Phys. **4**, 19 (2008).

[30]L. J. Chen, N. Bessho, B. Lefebvre, H. Vaith, A. Asnes, O. Santolik, A. Fazakerley, P. Puhl-Quinn, A. Bhattacharjee, Y. Khotyaintsev, P. Daly, and R. Torbert, Phys. Plasmas **16**, 056501 (2009).
[31]W. Daughton, J. D. Scudder, and H. Karimabadi, Phys. Plasmas **13**, 072101 (2006).
[32]C. Huang, Q. M. Lu, Z. W. Yang, M. Y. Wu, Q. L. Dong, and S. Wang, Nonlinear Process. Geophys. **18**, 727 (2011).
[33]C. Huang, Q. M. Lu, M. Y. Wu, S. Lu, and S. Wang, J. Geophys. Res. **118**, 991, doi:10.1002/jgra.50185 (2013).
[34]J. P. Eastwood, T. D. Phan, F. S. Mozer, M. A. Shay, M. Fujimoto, A. Retino, M. Hesse, A. Balogh, E. A. Lucek, and I. Dandouras, J. Geophys. Res. **112**, A06235, doi:10.1029/2006JA012158 (2007).
[35]M. Yamada, H. Ji, S. Hsu, T. Carter, R. Kulsrud, N. Bretz, F. Jobes, Y. Ono, and F. Perkins, Phys. Plasmas **4**, 1936 (1997).
[36]J. Egedal, A. Fasoli, M. Porkolab, and D. Tarkowski, Rev. Sci. Instrum. **71**, 3351 (2000).
[37]M. Yamada, Y. Ono, A. Hayakawa, M. Katsurai, and F. Perkins, Phys. Rev. Lett. **65**, 721 (1990).
[38]Y. Ono, A. Morita, M. Katsurai, and M. Yamada, Phys. Fluids B **5**, 3691 (1993).
[39]J. A. Stamper, E. A. McLean, and B. H. Ripin, Phys. Rev. Lett. **40**, 1177 (1978).
[40]P. M. Nilson, L. Willingale, M. C. Kaluza, C. Kamperidis, S. Minardi, M. S. Wei, P. Fernandes, M. Notley, S. Bandyopadhyay, M. Sherlock, R. J. Kingham, M. Tatarakis, Z. Najmudin, W. Rozmus, R. G. Evans, M. G. Haines, A. E. Dangor, and K. Krushelnick, Phys. Rev. Lett. **97**, 255001 (2006).
[41]C. K. Li, F. H. Seguin, J. A. Frenje, J. R. Rygg, R. D. Petrasso, R. P. J. Town, O. L. Landen, J. P. Knauer, and V. A. Smalyuk, Phys. Rev. Lett. **99**, 055001 (2007).
[42]W. Fox, A. Bhattacharjee, and K. Germaschewski, Phys. Rev. Lett. **106**, 215003 (2011).
[43]W. Fox, A. Bhattacharjee, and K. Germaschewski, Phys. Plasmas **19**, 056309 (2012).
[44]Q. L. Dong, S. J. Wang, Q. M. Lu, C. Huang, D. W. Yuan, X. Liu, X. X. Lin, Y. T. Li, H. G. Wei, J. Y. Zhong, J. R. Shi, S. E. Jiang, Y. K. Ding, B. B. Jiang, K. Du, X. T. He, M. Y. Yu, C. S. Liu, S. Wang, Y. J. Tang, J. Q. Zhu, G. Zhao, Z. M. Sheng, and J. Zhang, Phys. Rev. Lett. **108**, 215001 (2012).
[45]P. L. Pritchett, F. V. Coroniti, and R. Pellat, J. Geophys. Res. **96**, 11523, doi:10.1029/91JA01094 (1991).
[46]M. I. Sitnov, A. S. Sharma, P. N. Guzdar, and P. H. Yoon, J. Geophys. Res. **107**, 1256, doi:10.1029/2001JA009148 (2002).
[47]H. Karimabadi, W. Daughton, and K. B. Quest, Geophys. Res. Lett. **31**, L18801, doi:10.1029/2004GL020791 (2004).
[48]Q. M. Lu, S. Lu, C. Huang, M. Y. Wu, and S. Wang, Plasma Phys. Controlled Fusion **55**, 085019 (2013).
[49]F. F. Chen, *Introduction to Plasma Physics and Controlled Fusion* (Plenum Press, New York, 1984), p. 215.